Eva Rajo-Iglesias

Current Misuses and Future Prospects for Printed Multiple-Input, Multiple-Output Antenna Systems

Mohammad S. Sharawi

EDITOR'S NOTE

In this issue's "Wireless Corner" column, Prof. Sharawi discusses the major performance metrics for multiple-input, multiple-output (MIMO) antennas. The major misuses of some of these metrics are highlighted and common mistakes concerning design configurations are described. The article includes illustrative examples for each of the addressed problems. Finally, some future prospects of MIMO antenna system designs are given with special emphasis in the use of these systems in the millimeter-frequency range as well as in massive-MIMO architectures.

In the past six years or so, the number of scientific articles and conference papers providing possible multiple-input, multiple-output (MIMO) antenna system solutions has noticeably increased. Flagship conferences on antennas and propagation have recently had multiple sessions addressing MIMO antenna systems and their applications. The importance of such antenna systems lies in the magnitude of their application in current wireless devices and gadgets, and this thrust will continue because fourth-generation (4G) and the upcoming fifth-generation (5G) wireless standards rely heavily on MIMO technology. But throughout the years, and up until now, a wide range of publications still suffer from some major misconceptions and unclear understanding of the fundamental aspects while designing, characterizing, and evaluating such multiantenna systems.

In this article, I shine some light on a few of these fundamental issues and try to clarify them. Some examples from the literature are given to show the magnitude of such issues, and the goal is to try to avoid them in all future works. Finally, some prospects for the use of MIMO-based antenna systems in upcoming wireless standards and their enabling technologies are presented.

BACKGROUND

The design of MIMO antenna systems has been driven by the wireless industry as this technology is a major enabling one in 4G wireless standards and will continue as such in the upcoming 5G wireless standard. Using MIMO antenna systems is important because two of the parameters that can directly increase the channel capacity (i.e., give higher bit-rate transmissions) cannot be increased (within the current spectrum allocation by international operators, i.e., below 6 GHz). These parameters are the transmission bandwidth (BW) and power levels. The general-channel-capacity equation of M transmitter and N receiver antennas, with no channel-state information, Gaussian distributed signals, and identity covariance matrix is given by [1]

$$C = \mathrm{BW}\log_2\left(\det\left(\mathbf{I}_N + \frac{P_T}{\sigma^2 M}\mathbf{H}\mathbf{H}^H\right)\right), \qquad (1)$$

where C is the channel capacity (in bits/s), BW is the channel bandwidth (in hertz), min (N, M) is the minimum number of independent channels in the wireless environment, P_T is the equally distributed input power among the elements, σ^2 is the noise power, $\mathbf{I}_N$ is the $N \times N$ identity matrix, and $\mathbf{H}$ is the complex channel matrix. Equation (1) shows that an increase in BW or the signal-to-noise ratio yields a direct increase in C, but due to the limited spectrum bands as well as predefined power-level

Digital Object Identifier 10.1109/MAP.2017.2658346
Date of publication: 4 April 2017

transmissions set by governmental agencies and operators, these two factors are rarely available for any modifications. This leaves us with increasing M and N to achieve an increase in C, which is the main driver for MIMO systems.

The number of antenna elements needs to be increased at the base station side (large and small-sized ones, e.g., rooftop towers and indoor wireless access points) as well as at the user terminal (UT) side (e.g., handheld wireless terminals/devices). This increase is easy to accomplish on the base station side, but it is very challenging on the UT side. Despite that challenge, a large magnitude of designs and devices are already deployed in 4G equipment (e.g., cell phones, wireless access points, universal serial buses, and dongles) within the long-term evolution (LTE), wireless local area networks (WLAN), as well as Worldwide Interoperability for Microwave Access [2]. These 4G-enabled handheld devices currently have a maximum of two antennas operating at the same band(s) in a MIMO configuration. In addition, the number of antenna elements is expected grow from two up to eight in some handheld devices and wireless standards (e.g., 802.11ac) [2] to increase the data rates, but this poses some challenges to the antenna designer.

The characterization of MIMO antennas requires several metrics to be evaluated that have not been used in conventional single-input, single-output conventional wireless systems. These metrics such as the correlation coefficient (CC) or envelope CC (ECC), the total active reflection coefficient (TARC), the C, and multiplexing gain need to be evaluated as they give the designer an idea regarding the direct effect of the MIMO antenna system within the overall device capabilities in achieving the anticipated improvement. Thus, these metrics should be evaluated correctly. Several past works have provided detailed explanations for these metrics and have shown various examples and ways of implementing and applying them properly, such as in [2] and [3].

Even though there has been a steady increase in the number of published works in the area of MIMO antennas in recent years, several common misconceptions and misuses of metrics are widely spreading, and this invalidates the conclusions made in many studies. In addition, some of the proposed designs suffer from erroneous assumptions regarding their MIMO antenna geometries, while not considering the final product, thus limiting the practicality of the proposed designs. These common mistakes are sometimes overlooked by various review panels, thus giving the wrong impression to newcomers that these erroneous assumptions or misuses of such metrics are acceptable and valid in prestigious journals and conferences.

> **The number of antenna elements needs to be increased at the base station side (large and small sized ones, i.e., rooftop towers and indoors wireless access points) as well as at the user terminal side.**

The aim of this article is to identify such common misuses and misinterpretations that have been applied to printed-MIMO antenna systems (they are applicable to nonprinted systems as well) and to place them in context and give some correct guidelines for researchers. In addition, some future perspectives are given to what researchers could study regarding MIMO antenna designs for the upcoming and future wireless standards and devices driven by industrial forecasts.

SOME MISCONCEPTIONS/ MISUSES IN MIMO ANTENNA DESIGN

This section discusses several issues that need further clarification for their proper use in future designs and evaluations of MIMO antenna systems. They have been identified over the years as common mistakes that some recently published works still encounter.

NOT CONNECTED GROUNDS

This is a very common mistake that is still being practiced. Many authors tend to provide separate not-connected grounds (GNDs) for different antenna elements within a MIMO configuration, which is illustrated in Figure 1. For the sake of generality, simple printed monopole antennas are shown, but the idea can be applied to any type or antenna geometry. In Figure 1(a), the direct split in the GND plane can yield a direct enhancement in port isolation, and this is because there is be no current coupling through the GND plane since it is not continuous. This GND split is not practical since, in a real system, the signals should have a common reference plane, i.e., a single common GND plane, so that all signal levels within the system can be interpreted properly

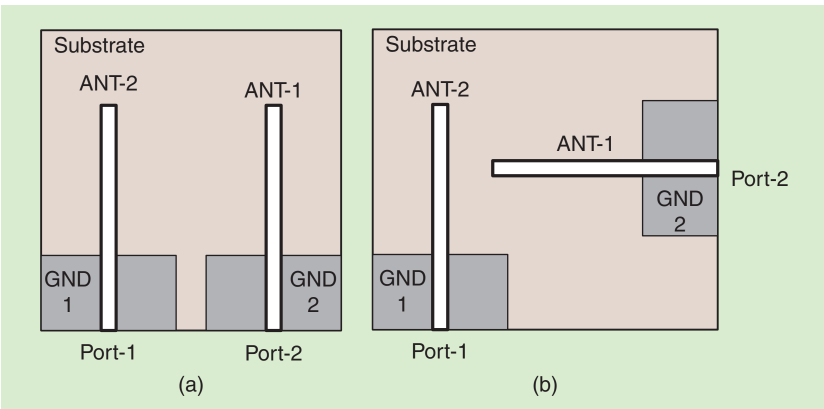

FIGURE 1. The separation of the GND planes of various antenna elements within MIMO configurations: (a) the same polarization and (b) orthogonal polarization.

based on that reference level (i.e., zero volts or GND level). If separate GND planes are used, one cannot guarantee that the system will work since the assumption of having all GND planes with the same voltage level is invalid [4]. Thus, providing MIMO antenna configurations with multiple GND planes should be avoided.

Figure 1(b) is most often used to provide an orthogonal polarization between the two MIMO antenna elements, but, again, the fact that two separate GND planes are used poses serious questions about whether this technique is practical, even though it might give good correlation coefficient values due to the pattern orthogonality achieved. In addition, the defected-ground-structure (DGS) technique that is usually used for enhancing port isolation in MIMO and multiantenna systems is still valid if the GND plane is not totally split. Several examples can be found in [2]–[6].

EVALUATION OF THE CC OR ECC

A very important parameter to evaluate for MIMO antenna systems is the CC or the ECC. This metric is important because it shows the amount of channel isolation in a wireless communication link. This channel isolation is important to achieve the anticipated improvement from (1). This means that if the channels are isolated (i.e., the CC = 0), the maximum C is achieved, while any values for the CC that are higher than zero (maximum of one) degrade the achieved channel capacity. The radiation patterns of the MIMO antenna system are used in the evaluation of the CC (ρ) or ECC (ρ_e), since they directly affect the channel between the transmitter and the receiver. In an isotropic channel [an isotropic or uniform channel is the one that has cross-polarization discriminator (XPR) = 1 and uniform incoming wave distributions, i.e., $P_\phi = P_\theta = 1/4\pi$], they can be evaluated according to [7]

$$|\rho_{12}|^2 = \rho_e(\text{ECC}) = \frac{\left|\iint_{4\pi} [E_1(\theta,\phi) * E_2(\theta,\phi)] d\Omega\right|^2}{\iint_{4\pi} |E_1(\theta,\phi)|^2 d\Omega \iint_{4\pi} |E_2(\theta,\phi)|^2 d\Omega}, \quad (2)$$

where $E_i(\theta,\varphi)$ is the complex three-dimensional (3-D) radiated field pattern for antenna $\boldsymbol{i}$. The expression in (2) is based on the assumption of having an isotropic wireless environment and this should always be highlighted. A more general expression that considers the environment effect is (3), which can be seen in the box at the bottom of the page, where XPR gives the ratio between the vertically polarized and horizontally polarized field components in the environment, $P_{\theta,\phi}(\Omega)$ is the wave distribution of the specific (ϕ,θ) angular directions, and $G_{\theta,\phi}(\Omega)$ is the gain (i.e., $G_\theta(\Omega) = E_\theta(\Omega)\, E_\theta(\Omega)^*$). In [8], a simplified relationship to find (2) based on the port parameters (S-parameters) for lossless-antenna systems was provided based on equating the powers in and out of the system. This relationship for a two-port-MIMO antenna system is given as (4), shown in the box at the bottom of the page.

Equation (4) has been commonly misused when the condition for it to be valid is ignored. Specifically, that condition is the assumption of using lossless antennas in an isotropic environment. Equation (4) should not be used when evaluating any lossy antenna. Unfortunately, there have been papers accepted where (4) is applied ignoring the aforementioned conditions. All printed antennas are lossy, and unless the efficiency of your proposed antenna is very high, then (4) should not be used to evaluate the CC or ECC in any work because it is not valid. This is a common issue that has been noticed in many works.

Another important issue is that port parameters have nothing to do with the channel behavior that is important for evaluating (1). This means that (4) should not be used to evaluate the CC or ECC even for 100%-efficient-MIMO antenna systems, but (2) or (3) are rather the ones that directly connect the antenna-spatial behavior with that of the channel. The radiation patterns of adjacent similar lossless antennas give very high correlation when (2) or (3) are used compared to using (4), which gives very low CC/ECC values due to the low coupling between them. This can be easily proven via simulations as shown later in this section, and this was shown via experiments directly showing the channel capacity effect when obtaining highly efficient monopole antennas closer together—increasing correlation via spatial separation—in [9] and as an analytical consequence in [10]. This poses a major issue when using (4) instead of (2) or (3). In early works, obtaining the 3-D patterns was claimed to be difficult or time consuming, and the MIMO community was new to the various parameters and their evaluation and valid conditions. But now this is not the case, and (4) should not be used since it does not have any connection with the channel or the spatial behavior of the antennas, even though getting measured patterns at various frequencies can require more time than processing the S-parameter curves, but

$$|\rho_{12}|^2 \approx \rho_{e12} = \left| \frac{\oiint \text{XPR} \times E_{\theta i}(\Omega) E^*_{\theta j}(\Omega) P_\theta(\Omega) + E_{\varphi i}(\Omega) E^*_{\varphi j}(\Omega) P_\varphi(\Omega) d\Omega}{\sqrt{\oiint \text{XPR} \times G_{\theta i}(\Omega) P_\theta(\Omega) + G_{\varphi i}(\Omega) P_\varphi(\Omega) d\Omega}\sqrt{\oiint \text{XPR} \times G_{\theta j}(\Omega) P_\theta(\Omega) + G_{\varphi j}(\Omega) P_\varphi(\Omega) d\Omega}} \right|, \quad (3)$$

$$\rho_{12} = \left| \frac{|S_{11}{}^* S_{12} + S_{21}{}^* S_{22}|}{[(1-(|S_{11}|^2 + |S_{21}|^2))(1-(|S_{22}|^2 + |S_{12}|^2))]^{\frac{1}{2}}} \right|. \quad (4)$$

this process has become much faster compared to when initial works were published (especially using the new near-field based systems). Thus, considering the port power values only without considering the radiated field orientations has become an issue when evaluating the CC/ECC.

The way that MIMO antenna system designers should approach improving the CC/ECC is to spatially isolate the radiation patterns. This can be done by using different polarizations, or tilted beams (e.g., via beam steering, use of reflectors within the GND, and use of parasitic directors). Several examples are already out there such as those in [11]–[13], but it should be emphasized again.

In addition, three other methods have been proposed in the literature that consider the lossy behavior of printed antennas when finding the CC or ECC from port parameters in [14]–[16] in isotropic environments. In [14], the effect of antenna efficiency was incorporated into the expression from (4) as an upper bound, but the values become unrealistic for lossy antennas with values less than 50%. Thus, its applicability is limited due to the over estimation of the CC/ECC values. A systematic method was proposed in [15] to incorporate the effect of losses within (4) by adding a lossy element and embedding its effect. The method gave close agreement with the radiation pattern method (2), but it was applied on some basic-antenna elements (i.e., dipoles and patches), and its accuracy can deteriorate if the elements are placed unsymmetrical with respect to one another, thus needing further investigation. Finally, the method in [16] showed limited applicability due to the specificity of the method for the specific decoupling network provided. A detailed comparison for the three methods will be presented in a follow-up article, and thus the methods are not discussed any further here. The focus in this article is on the basic misuse of the *S*-parameter method because of lossless assumptions that is becoming a common issue in recent works proposing MIMO antenna structures as well as considering beam tilting to spatially isolate the MIMO channels.

Getting measured patterns at various frequencies can require more time than processing the *S*-parameter curves, but this process has become much faster compared to when initial works were published.

MIXUP BETWEEN PORT-ISOLATION AND FIELD CORRELATION

The discussion of this mix-up, isolation versus correlation, agrees with the previous clarification provided in the "Evaluation of the CC or ECC" section. Port isolation via the enhancement of Sxy has nothing to do with the radiated fields that are the actual contributors to the channel correlations. The reduction of coupling between the input ports is denoted as port-isolation enhancement. Although many works that already appear in literature claimed that enhancing port isolation enhances the correlation coefficient according to the incorrect use of (4), there are no direct connections between port coupling and the radiated fields, as most coupling occurs through the ground (except lower efficiency or radiated power). Thus, this claim is questionable. Enhancing the port isolation enhances the system efficiency via increasing the power that is delivered to the antenna.

Although a radiated field from antenna 1 can be detected by an adjacent antenna (antenna 2) as an induced voltage at its input port, this does not alter the actual field transmitted by antenna 1. This affects the radiation efficiency as part of the radiated fields were captured by a nearby antenna and not sent to space. Thus, if we look at the original radiated fields for antenna 1 in the presence of antenna 2 and antenna 2 in the presence of antenna 1, adding a port-isolation-enhancement structure (i.e., a port-decoupling network) does not alter the radiation patterns (unless the patterns are already affected by the adjacent radiator acting as a reflector due to its close placement); thus, the CC/ECC calculated from (2) via the radiated fields does not change [17].

ILLUSTRATIVE EXAMPLES

Two examples are investigated to clarify the issues mentioned in the previous sections.

EXAMPLE 1

Take a two-element patch-based-MIMO antenna example as shown in Figure 2. The model was simulated using HFSS V15, and the *S*-parameters and the complex radiated fields were extracted. The radiation efficiency was about 50% [an epoxy-glass 4 (FR4) substrate with a dielectric constant of 4 and a thickness of 0.8 mm]. The obtained *S*-parameter curves are shown in Figure 2(b), and the radiated fields (realized gain patterns) are shown in Figure 2(c). The calculated CC curves using (2) (with legend using *S*-parameters) and (3) (with legend using Far Field) are shown in Figure 2(d). Note the large discrepancy between the two even with isolation levels higher than 20 dB. Thus, higher isolation does not mean better correlation coefficients.

EXAMPLE 2

A four-element-MIMO antenna system is also investigated, as shown in Figure 3. The antenna consists of four monopole-like antenna elements covering the bands 1.97–2.19 GHz. The MIMO antenna system occupies the edges of a standard mobile phone terminal with $60 \times 100 \times 0.8$ mm^3 size and built on an FR4 commercial substrate. The measured and simulated *S*-parameters are shown in Figure 4(a), and the simulated 3-D patterns are shown in Figure 4(b). The isolation levels are around the –11 dB for the worst-case scenario, and the simulated efficiency was more than 85%. The CC curves were obtained using the *S*-parameter method (4) in Figure 5(a) and the field based method (2) in Figure 5(b). Thus, the *S*-parameter method fails to predict the correct values for the CC even for good-efficiency antennas with high-coupling levels. In addition, the tilted

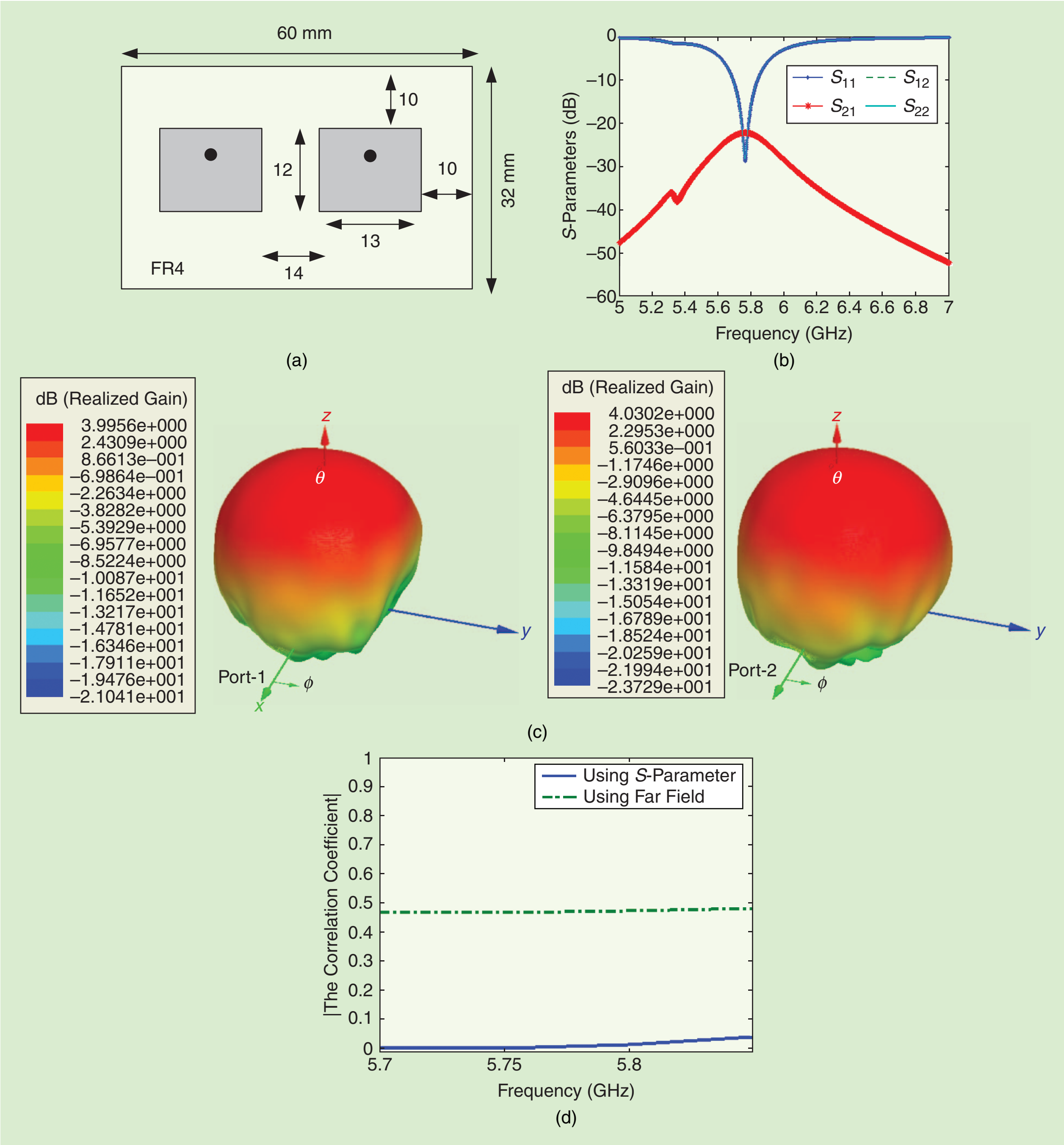

FIGURE 2. A two-element-patch-based MIMO antenna example: its (a) geometry, (b) simulated *S*-parameters, (c) simulated 3-D gain patterns, and (d) CC curves.

beams due to the presence of the GND plane acting as a reflector provides good correlation values.

AN ADDITIONAL NOTE

Additionally, when enhancing the port isolation via a DGS or a parasitic element within a printed-MIMO antenna system, for example, the placement of the isolation-enhancement structure between the two radiating elements on a specific substrate ends up tilting the radiation pattern due to the presence of a reflector behind it or the change in the current distribution around it, and this explains some of the enhancements achieved when using (2) after utilizing a certain DGS or any other isolation enhancement method. However, the majority of works are mixing the use of (4) along with the misinterpretation and connection between port isolation and field correlation, thus giving the conclusion that enhancing the port isolation (or coupling via enhancing S_{xy}) will yield enhanced CC or ECC values. Extreme care should be taken in this regard. I have avoided listing examples from literature, due to the sensitivity of the issue, but the reader is urged

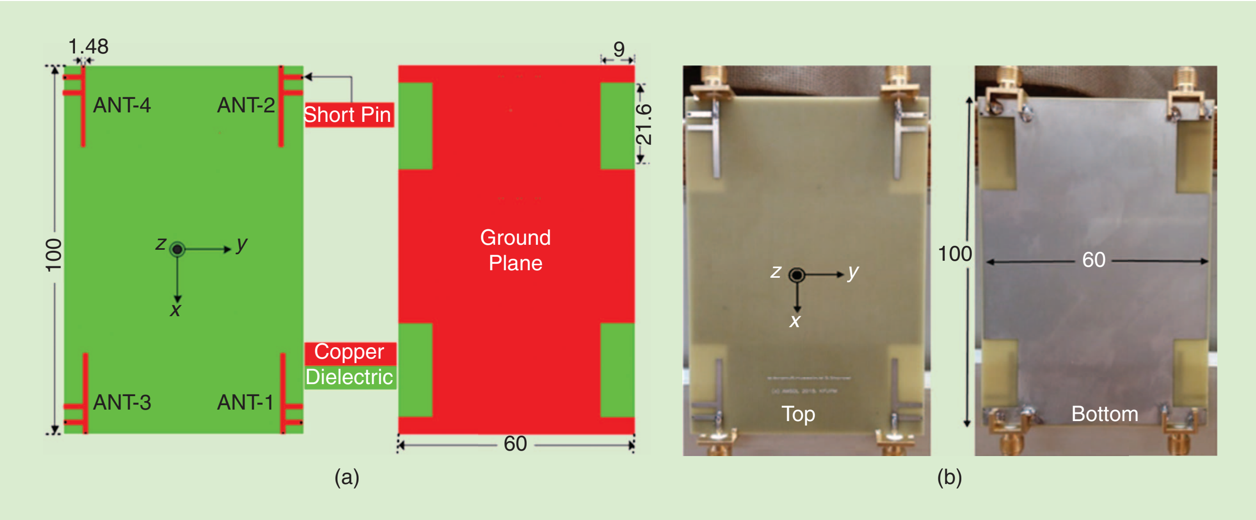

FIGURE 3. A four-element modified printed-monopole-based MIMO antenna example: its (a) geometry and (b) fabricated prototype.

to take a closer look and verify this on several old and recent works. Port isolation might also lead to noticeable field-correlation enhancement where the orientation of the MIMO antennas are such that the patterns become orthogonal and the ports are placed 90° with respect to one another [e.g., similar to what is shown in Figure 1(b)]. The orthogonality between the GND currents as well as the radiated fields can also give the enhancement in both at the same time, but continuous GND planes should always be used.

WHAT IS NEXT IN THIS AREA?

The demand for higher data rates and video-on-demand will not slow down in the coming years. The 5G standard is expected to provide at least 1,000 times faster data rates compared to 4G. Although a standard for 5G has not been established, various entities around the world are discussing the standardization and frequencies to be used. Several enabling technologies will be devised, and this section discusses a few of them from the antenna design perspective, where all of them are MIMO-based ones.

RECONFIGURABLE MIMO ANTENNAS FOR COGNITIVE RADIOS

Cognitive radios (CRs) are intelligent radios that can sense their environment and intelligently switch between

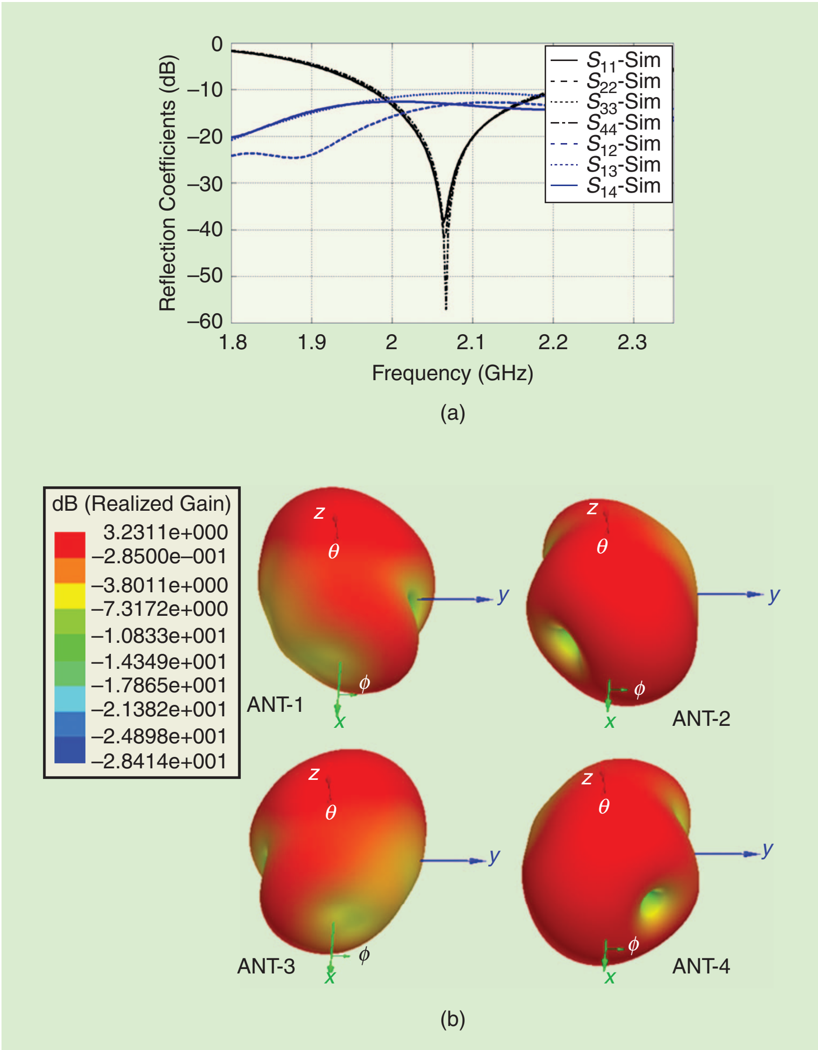

FIGURE 4. The measured and simulated results for the four-element monopole like MIMO antenna system in Figure 3: its (a) port parameters and (b) simulated 3-D patterns.

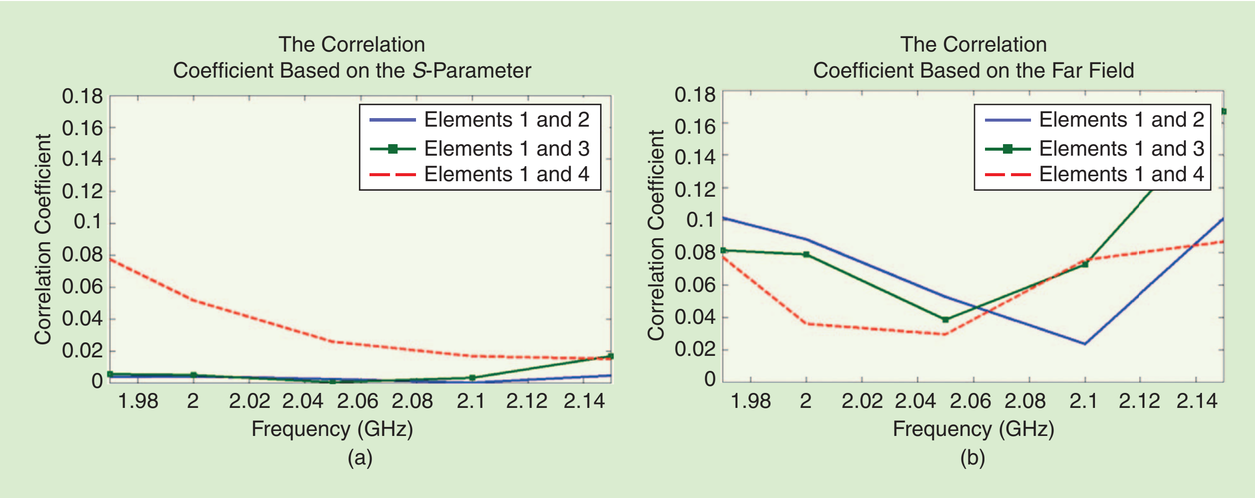

FIGURE 5. The calculated CC values from measured quantities, (a) using the *S*-parameter method utilizing (4) and (b) using the 3-D patterns utilizing (2).

underutilized frequency bands. The concept of a cognitive radio was first proposed by J. Mitola in 1998 [18]. Wide-band- and frequency-reconfigurable antennas are needed for CR platforms. Moving toward dynamic spectrum sensing and efficient spectrum utilization has been the center of technological thrusts and forums such as that in [19], where major challenges for the implementation of the second-generation CR platform were discussed. From industrial perspectives, software-defined radio platforms that utilize programmable radio-frequency (RF) front ends with MIMO capabilities are a major player in pushing for such reconfigurable antenna systems [20], [21]. Few implementations of MIMO-based reconfigurable CR antenna systems have recently appeared in literature such as those in [22]–[24]. All of which consisted of a dedicated sensing antenna that has ultrawideband (UWB) capabilities, and a dedicated MIMO antenna system (consisting of two elements). In [22], a two-element reconfigurable MIMO and sensing antenna was proposed for CR applications. The size of the complete system was 80 × 70 × 1.6 mm^3, and the sensing antenna covered a range of 3–6 GHz while the MIMO antennas covered three bands around 4 GHz. Each antenna within the system had a separate GND.

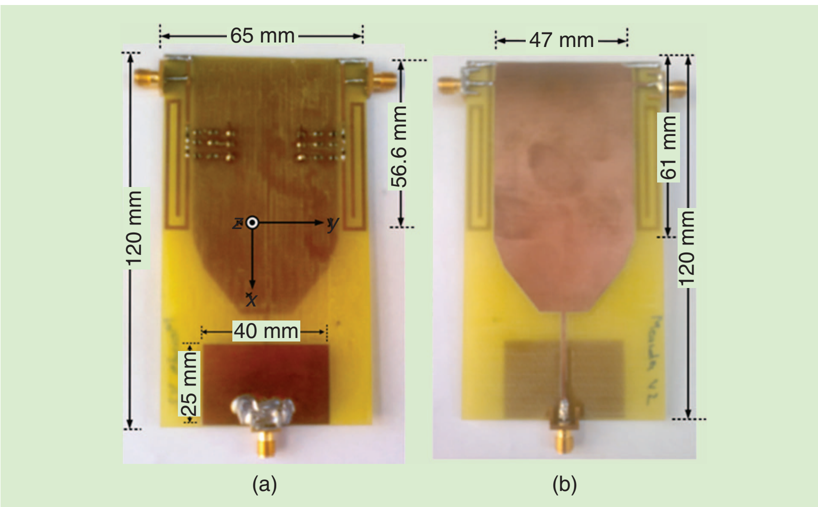

FIGURE 6. A reconfigurable MIMO and UWB-sensing antenna for CR applications from [23]: (a) a top view and (b) a bottom view.

In [23] and [24], integrated reconfigurable MIMO and sensing antennas were proposed. The GND plane of the MIMO antenna system was used as the UWB-sensing antenna. The UWB sensing antenna covered a range of 0.7–3 GHz, while the MIMO antennas switched bands using varactor and p-i-n diodes within 0.8–2.5 GHz. The size of these integrated antennas was 65 × 120 × 0.8 mm^3. Printed inverted-F antennas (PIFAs) and meandered-PIFA based elements were used, and Figure 6 shows the proposed fabricated antenna in [23].

MILLIMETER-WAVE MIMO ANTENNA SYSTEMS

The 5G standard establishes a large increase in the data throughput, where an increase of 1,000 times is expected in the overall theoretical channel capacity. This increase relies on several enabling technologies in 5G, one of which is the use of the millimeter-wave spectrum where excess BW can be utilized [according to (1), more BW means direct increase in *C*]. Although a standard has not been established for 5G wireless technology, several players around the world are investigating various bands in the mm-wave spectrum as potential candidates for such a technology. Such bands include the 28, 38, 40, 60, and 70 GHz [25]. The 28- and 38-GHz bands have been recently investigated for cellular communications, and promising results were revealed showing that the use of cellular communication terminals can be possible even at 28 GHz with good reliability [26]. Of course, to have the highest throughput, the mobile terminal should be close to the base station. MIMO is also an enabling technology for 5G as well as massive-MIMO, which is discussed in the "Massive MIMO Antenna Systems" section.

The literature in this area is very limited, but more work is underway as several groups around the world are working on mm-wave MIMO antenna systems for 5G terminals. One example is presented in [27] where a 30-GHz based dual-element-based MIMO antenna was proposed with at least 1 GHz of BW. Each element of the MIMO antenna system consists of a linear array of four cylindrical-dielectric-resonator antennas (cDRA). The array of four elements had a special feed network with a fixed-progressive phase that is used to tilt the beam by 45°, while the other port beam is tilted toward –45°. This is used to improve the CC and enhance the channel isolation to achieve the MIMO advantage and spatial multiplexing. The gain of the complete system including the feed network losses was approximately 8 dBi (per port). The MIMO antenna system was compact with antenna dimensions of $46 \times 10 \times 3.2$ mm^3 (including the GND plane of the antenna array). Such a system can be placed on the edges of a 5G terminal and a photograph of the fabricated prototype is shown in Figure 7.

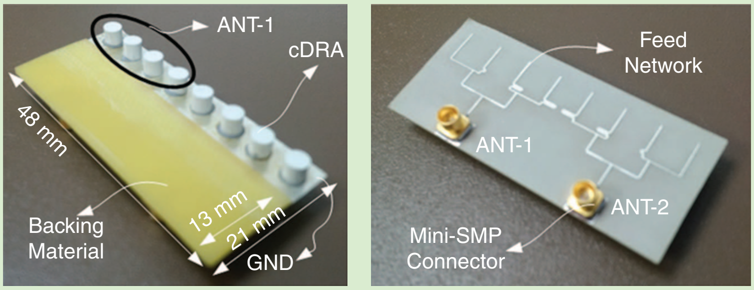

FIGURE 7. An mm-wave MIMO antenna system based on cDRA arrays: (a) a top view and (b) a bottom view.

MASSIVE MIMO ANTENNA SYSTEMS

The use of a large MIMO antenna system is denoted as massive MIMO, or large-scale MIMO. Using a large number of antenna elements at the base station side (of course due to the abundance of spatial space)—on the order of tens to hundreds—has several advantages on the wireless communication system such as increasing the number of independent channels, and thus increasing the system capacity; providing higher transmission efficiency due to the use of narrower dedicated beams to various users; providing higher signal to noise ratios and lower interference levels; in addition to the use of inexpensive low-power components (since the power is divided, more gain is achieved from the operation of groups of elements) [28]. Massive-MIMO is a technology that is being investigated heavily for future use in 5G wireless systems.

Focusing on the antenna implementation, antenna-system solutions for massive-MIMO are still considered very limited, and the proposed structures from industry and academia are still small compared to those for MIMO, since the standard for 5G has not been established. Some of the recent works in massive-MIMO antenna systems are evident in [29]–[31]. (The list is not complete here and only a few examples are given. However, the reader can easily prove for her/himself that only a handful of antenna systems for massive-MIMO exist.) In [29], a massive-MIMO antenna system implementation was devised by Samsung Inc. The antenna system consisted of 8×4 planar arrays of four-patch antenna elements in each subarray (total of 128 antennas, but each four patches act as a single element). The antenna array operated in the LTE 2.5–2.6-GHz bands with narrow beamwidth and high isolation. In [30], another planar-patch-antenna-based massive-MIMO antenna array was proposed along with its test bed. It operated at a 3.7-GHz band with 100 elements arranged in a T-shape, and almost a 180-MHz BW was achieved. This was a joint collaboration between Lund University and National Instruments (see Figure 8). Finally, a cylindrical-shaped massive-MIMO antenna system was proposed by Xilinx Inc. (called MegaBee) that can cover 4G bands and was scaled up to 256 elements in [31].

Having mm-wave-based massive-MIMO architectures and antenna systems has been projected in recent literature to operate within the 5G umbrella as discussed in [32]–[34]. There are several challenges that need to be addressed in terms of the propagation channel modeling, hardware integration and antenna system development, but the potential has been identified. In [34], the work focused on the channel modeling aspect of such systems, thus opening the door for antenna system implementations that provide novel solutions to integration with microwave and legacy 4G antenna systems at the base-station side.

FIGURE 8. A 100-element massive-MIMO antenna system and test bed [30].

Some challenges in the implementation of such massive-MIMO antenna systems include careful design of the RF front ends that aid in the multiuser beamforming capabilities of such dense arrays, in addition to the hardware integration issues. Some of the potential challenges when considering mm-wave massive-MIMO systems for short-range communications are the hardware integration issues encountered when considering the RF front ends and the size of such pico and femto cells. Consequently, antenna designs for massive-MIMO at both microwave as well as mm-wave bands need close attention from the research community.

CONCLUSIONS

In this article, some major misuses of some MIMO antenna performance metrics as well as design configurations were highlighted so that future designs can be certain that these issues are avoided and approached/used in the proper way, and several examples were given for illustration only. Specifically, the calculation of the correlation coefficient between MIMO antenna elements should be done always using the field equation. Also, no split in the system GND plane should be used in any future design, as this does not make any practical sense. Finally, the article concludes with some future prospects of MIMO antenna-system designs in CR applications and 5G wireless standards via the utilization of mm-wave bands and massive-MIMO architectures.

ACKNOWLEDGMENTS

This work was supported by the Deanship of Scientific Research at King Fahd University of Petroleum and Minerals under project number RG1419. I would like to thank Abdelmoniem Hassan and Muhammad Ikram for generating some of the figure plots.

AUTHOR INFORMATION

Mohammad S. Sharawi (msharawi@kfupm.edu.sa) is a professor of electrical engineering at King Fahd University of Petroleum and Minerals, Dhahran, Saudi Arabia. He is the founder and director of the Antennas and Microwave Structure Design Laboratory, and he is a Senior Member of the IEEE and a fellow of the Intuition of Engineering and Technology.

REFERENCES

[1] A. Goldsmith, *Wireless Communications.* Cambridge, MA: Cambridge Univ. Press, 2005.
[2] M. S. Sharawi, *Printed MIMO Antenna Engineering.* Norwood, MA: Artech House, 2014.
[3] M. S. Sharawi, "Printed multi-band MIMO antenna systems and their performance metrics," *IEEE Antennas Propag. Mag.*, vol. 55, no. 5, pp. 218–232, 2013.
[4] S. H. Hall and H. L. Heck, *Advanced Signal Integrity for High-Speed Digital Designs.* Hoboken, NJ: Wiley, 2009.
[5] H. Li, J. Xiong, and S. He, "A compact planar MIMO antenna system of four elements with similar radiation characteristics and isolation structure," *IEEE Antennas Wireless Propag. Lett.*, vol. 8, pp. 1107–1110, 2009.
[6] X. Zhou, X. Quan, and R. L. Li, "A dual-broadband MIMO antenna system for GSM/UMTS/LTE and WLAN handsets," *IEEE Antennas Wireless Propag. Lett.*, vol. 11, pp. 551–554, 2012.
[7] R. G. Vaughan and J. B. Andersen, "Antenna diversity in mobile communications," *IEEE Trans. Veh. Technol.*, vol. 36, no. 4, pp. 149–172, 1987.
[8] S. Blanch, J. Romeu, and I. Corbella, "Exact representation of antenna system diversity performance from input parameter description," *Electron. Lett.*, vol. 39, no. 9, pp. 705–707, 2003.
[9] D. W. Browne, M. Manteghi, M. P. Fitz, and Y. Rahmat-Samii, "Experiments with compact antenna arrays for MIMO radio communications," *IEEE Trans. Antennas Propag.*, vol. 54, no. 11, pp. 3239–3250, Nov. 2006.
[10] S. Mikki and Y. M. M. Antar, "On cross correlation in antenna arrays with applications to spatial diversity and MIMO systems," *IEEE Trans. Antennas Propag.*, vol. 63, no. 4, pp. 1798–1810, 2015.
[11] S. Park and C. Jung, "Compact MIMO antenna with high isolation performance," *Electron. Lett.*, vol. 46, no. 6, pp. 390–391, 2010.
[12] S. Dhar and M. S. Sharawi, "A UWB semi-ring MIMO antenna with isolation enhancement," *Microwaves Opt. Technol. Lett.*, vol. 57, no. 8, pp. 1941–1946, 2015.
[13] J. F. Valenzuela-Valdes, M. A. Garcia-Fernandez, A. M. Martinez-Gonzalez, and D. A. Sanchez-Hernandez, "Evaluation of true polarization diversity for MIMO systems," *IEEE Trans. Antennas Propag.*, vol. 57, no. 9, pp. 2746–2755, Sept. 2009.
[14] P. Hallbjorner, "The significance of radiation efficiencies when using the *S*-parameters to calculate the received signal correlation from two antennas," *IEEE Antennas Wireless Propag. Lett.*, vol. 4, pp. 97–99, 2005.
[15] H. Li, X. Lin, B. K. Lau, and S. He, "Equivalent circuit based calculation of signal correlation in lossy MIMO antennas," *IEEE Trans. Antennas Propag.*, vol. 61, no. 10, pp. 5214–5222, 2013.
[16] K. Wang and T. Eibert, "Estimation of signal correlation of lossy compact monopole arrays in decoupling networks," *IEEE Trans. Antennas Propag.*, vol. 63, no. 1, pp. 357–363, 2015.
[17] S. C. Chen, Y. S. Wang, and S. J. Chung, "A decoupling technique for increasing the port isolation between two strongly coupled antennas," *IEEE Trans. Antennas Propag.*, vol. 56, no. 12, pp. 3650–3658, Dec. 2008.
[18] J. Mitola, "Cognitive radio architecture evolution," *Proc. IEEE*, vol. 97, no. 4, pp. 626–641, 2009.
[19] National Science Foundation. (2010). Workshop on enhancing access to the radio spectrum (EARS). [Online]. Available: http://www.nsf.gov/mps/ast/nsf_ears_workshop_2010_final_report.pdf
[20] Nutaq Innovations. [Online]. Available: http://www.nutaq.com/
[21] National Instruments. [Online]. Available: http://www.ni.com/
[22] Y. Tawk, J. Costantine, and C. Christodoulou, "A MIMO cognitive radio antenna system," in *Proc. IEEE Int. Conf. Antennas and Propagation (APS/Union Radio Sci.)*, 2013, pp. 572–573.
[23] R. Hussain and M. S. Sharawi, "A cognitive radio reconfigurable MIMO and sensing antenna system," *IEEE Antennas Wireless Propag. Lett.*, vol. 14, pp. 257–260, 2015.
[24] R. Hussain and M. S. Sharawi, "An integrated reconfigurable MIMO antenna system with an UWB sensing antenna for cognitive radio platforms," *IET Microwaves, Antennas Propag.*, vol. 9, no. 9, pp. 940–947, June 2015.
[25] Quotient Associates. (2015, March). "5G candidate band study," Final report to ofcom. [Online]. Available: http://stakeholders.ofcom.org.uk/binaries/consultations/above-6ghz/qa-report.pdf
[26] T. S. Rappaport, S. Sun, R. Mayzus, H. Zhao, Y. Azar, K. Wang, G. N. Wong, J. K. Schulz, M. Samimi, and F. Gutierrez, "Millimeter wave mobile communications for 5G cellular: It will work!," *IEEE Access*, vol. 1, pp. 335– 349, 2013.
[27] M. T. Hussain, O. Hammi, M. S. Sharawi, S. Podilchak, and Y. M. M. Antar, "A dielectric resonator based millimeter-wave MIMO antenna array for handheld devices," in *Proc. IEEE Antennas and Propagation Society Int. Symp. (APS/Union Radio Sci. 2015)*, July 2015, pp. 3–4.
[28] E. G. Larsson, O. Edfors, F. Tufvesson, and T. L. Marzetta, "Massive MIMO for next generation wireless systems," *IEEE Commun. Mag.*, vol. 52, no. 2, pp. 186–195, 2014.
[29] I. Tzanidis, B. L. Ng, Y. Li, Y.H. Nam, G. Xu, J. Zhang, Y. Kim, and J. Lee, "Patch antenna array configuration for application in FD-MIMO systems", in *Proc. IEEE Antennas and Propagation Society Int. Symp. (APS/Union Radio Sci.)*, July 2013, pp. 2241–2242.
[30] J. Vieira, S. Malkowsky, K. Nieman, Z. Miers, N. Kundargi, L.Liu, I. Wong, V. Owall, O. Edfors, F. Tufvesson, "A flexible 100-antenna testbed for Massive MIMO," in *Proc. IEEE Globecom Workshops*, Dec. 2014, pp. 287–293.
[31] CIOReview. (2015, Feb. 27). Xilinx and Mega-Bee launch prototyping platforms for 5G massive MIMO antenna systems. *CIOReview*. [Online]. Available: http://telecom.cioreview.com/news/xilinx-and-megabee-launch-prototyping-platform-for-5g-massive-mimo-antenna-systems-nid-5344-cid-39.html
[32] J. G. Andrews, S. Buzzi, W. Choi, S. V. Hanly, A. Lanzano, A. C. K. Soong, and J. C. Zhang, "What will 5G be?" *IEEE J. Sel. Areas Commun.*, vol. 32, no. 6, pp. 1065–1082, June 2014.
[33] L. Lu, G. Y. Li, A. Lee Swindlehurst, A. Ashikhmin, and R. Zhang, "An overview of massive MIMO: Benefits and challenges," *IEEE J. Select. Topics Signal Process.*, vol. 8, no. 5, pp. 742–758, Oct. 2014.
[34] S. Montagner, N. Benvenuto, and S. Tomasin, "Taming the complexity of mm-wave massive MIMO systems: Efficient channel estimation and beamforming," in *Proc. IEEE Int. Communications Conf. (ICC)*, London, June 2015, pp. 1251–1256.